

# Lawrence Berkeley National Laboratory

## Recent Work

**Title**

ARC SPECTRUM OF MAGNESIUM OXIDE

**Permalink**

<https://escholarship.org/uc/item/3z89g1j2>

**Author**

Green, David W.

**Publication Date**

1968-02-01

eg. 2

# University of California

## Ernest O. Lawrence Radiation Laboratory

ARC SPECTRUM OF MAGNESIUM OXIDE

David W. Green  
(Ph.D. Thesis Part II)

February 1968

**TWO-WEEK LOAN COPY**

*This is a Library Circulating Copy  
which may be borrowed for two weeks.  
For a personal retention copy, call  
Tech. Info. Division, Ext. 5545*

Berkeley, California

UCRL-17878 Rev.  
eg. 2

UNIVERSITY OF CALIFORNIA  
Lawrence Radiation Laboratory  
Berkeley, California  
AEC Contract No. W-7405-eng-48

ARC SPECTRUM OF MAGNESIUM OXIDE

David W. Green

(Ph.D. Thesis Part II)

February 1968

CONTENTS

ABSTRACT

I	INTRODUCTION . . . . .	1
II	THEORETICAL PREDICTIONS . . . . .	7
	A. Expected Electronic States . . . . .	7
	B. Computer Program . . . . .	16
III	EXPERIMENTAL . . . . .	17
	A. Spectrographs and Photographic Materials . . . . .	17
	B. Magnesium Oxide Vacuum Arc . . . . .	19
	C. Measurement of Plates . . . . .	22
IV	RESULTS . . . . .	23
	A. $C^1\Sigma^- - A^1\Pi$ and $D^1\Delta - A^1\Pi$ Band Heads . . . . .	23
	B. New Violet Band Systems . . . . .	34
	C. Ultra-violet Band Systems . . . . .	40
	D. Triplet Considerations . . . . .	42
V	CONCLUSIONS . . . . .	45
	A. Violet Band Heads . . . . .	45
	B. Identification of Triplets . . . . .	48
	REFERENCES . . . . .	50
	ACKNOWLEDGEMENTS . . . . .	53
	APPENDIX A - Program "Heads" . . . . .	54
	APPENDIX B - Program "Stand" . . . . .	59

ARC SPECTRUM OF MAGNESIUM OXIDE

David W. Green

Inorganic Materials Research Division, Lawrence Radiation Laboratory,  
and Department of Chemistry, University of California  
Berkeley, California

ABSTRACT

A comparison of the observed molecular electronic states of magnesium oxide is made to the states predicted by theoretical considerations. The observations reported are incomplete and considerable uncertainty exists about the states below 10 kK ( $10,000 \text{ cm}^{-1}$ ). Low-lying triplet states are predicted on the basis of atomic states of the separated atoms and semi-empirical molecular orbital considerations.

Assignments are made to a number of observed but previously unassigned band heads in the violet spectrum of MgO. The (0,0) sequences of the  $C^1\Sigma^- - A^1\Pi$  and  $D^1\Delta - A^1\Pi$  transitions as well as the (0,1) sequence of the  $D^1\Delta - A^1\Pi$  have been observed in the arc spectrum of magnesium oxide.

Additional band systems with sequences beginning at 3672 and 3637 Å have been observed and measured. Band heads are observed in the region from 2600-2800 Å which cannot be attributed to a known transition.

The possible assignment of the C and D states of magnesium oxide to triplets is considered. Relative intensities of the violet, green and red band systems of MgO are reported. Second differences for the C and D states are calculated from the previously reported rotational lines. Intensity calculations are performed for the branches of a  $^3\Sigma^- - ^3\Pi$  electronic transition with the  $^3\Pi$  state intermediated between Hund's coupling cases a) and b). No clear conclusions are drawn about the location of electronic triplet states in the MgO molecule.

## I. INTRODUCTION

The study of equilibrium and non-equilibrium high temperature systems is of increasing importance. Astronomical mechanisms of stellar and planetary evolution require a knowledge of the thermochemical behavior of high-temperature systems in order to explain observed spectra. The exploration of the upper terrestrial atmosphere and outer space requires thermodynamic data and a knowledge of vaporization processes for such problems as atmospheric re-entry and metallic resistance to oxidation.

Accurate thermodynamic functions allow the calculation of equilibrium behavior over large temperature ranges. The relative abundances of all constituents of a vapor system as a function of temperature would be known if the thermodynamic data were complete. Some systems have been well characterized, but many important systems are uncertain due to inadequate data.

High temperature vaporization processes can become complex due to multiple competing reactions. The magnesium oxide solid-vapor equilibrium is an example of such a system. The calculated vapor phase composition at high temperatures is extremely sensitive to the thermodynamic properties of the various species.

Generally atomic properties are well-known. Diatomic molecular properties are amenable to study by spectroscopic means. A knowledge of the molecular energy levels allows the calculation of the molecular partition function from which all the thermodynamic properties may be derived. For many molecules the known energy levels, although far from complete, are sufficient to determine the thermodynamic functions over temperature ranges of interest. This is true generally for diatomic molecules formed from the first row of the periodic table. For diatomic molecules formed from transi-

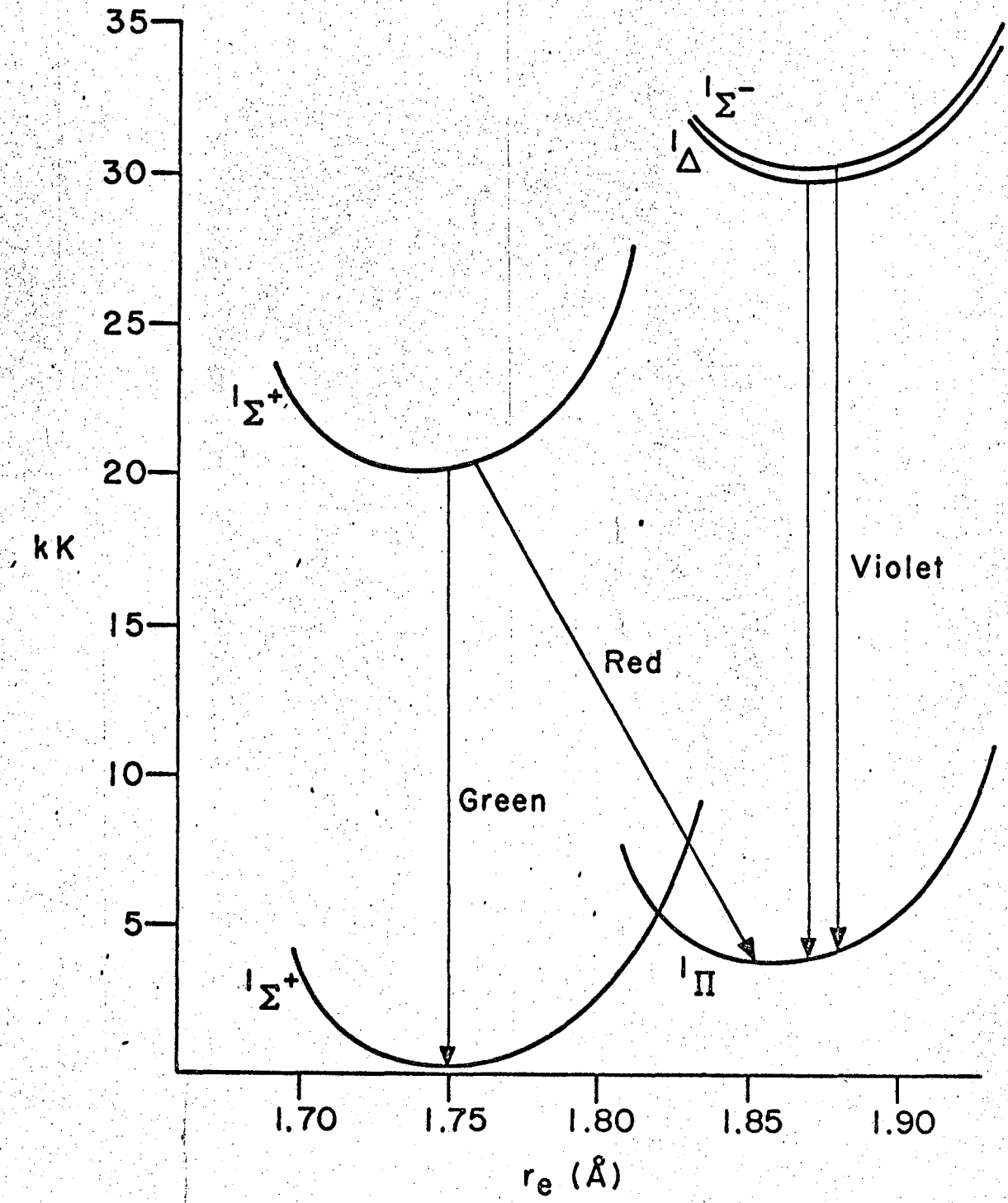
tion metals, only a few of the many expected low-lying molecular energy levels have been spectroscopically observed. In fact, the electronic ground state is not unambiguously known in most cases.

Polyatomic species require considerably more spectral analysis in order to determine their thermodynamic properties accurately. Relatively few molecules have been adequately analyzed.

Vapor systems of alkaline earth oxides, especially MgO, have been studied.<sup>1-3</sup> Yet considerable uncertainty still exists in large part due to incomplete knowledge of the alkaline earth oxide diatomic vapor properties.

The spectra of the alkaline earth oxides are of interest partially because they are so incomplete. For example, the MgO molecule has a red spectrum<sup>4-7</sup> attributed to  $B^1\Sigma^+ - A^1\Pi$ , a green spectrum<sup>4-11</sup> attributed to  $B^1\Sigma^+ - X^1\Sigma^+$  and a complex violet spectrum. At least two emitters give band heads in the region from 3600 Å to 4000 Å, namely MgO and MgOH. Extensive overlap has made early analyses difficult and only unassigned band heads have been reported.<sup>2,9,12-18</sup> Recently high resolution studies<sup>19,20</sup> have assigned two MgO electronic transitions within the violet region. The lower state is  $A^1\Pi$  and the upper states have been assigned as  $C^1\Sigma^-$  and  $D^1\Delta$ . Figure 1 shows the states which give rise to these transitions.

No triplet system has been assigned for MgO despite the prediction of several low-lying triplet states.<sup>21,22</sup> It is possible that MgO has a triplet ground state.<sup>21</sup> Probably the triplet states are low enough in energy to raise the possibility that the large electronic degeneracy of the triplet states could dominate the electronic partition function and have a considerable effect on the thermodynamic free-energy function of MgO. The partition function and resultant thermodynamic properties of MgO are sub-



XBL 682-116

Fig. 1. Known magnesium oxide electronic states and transitions.



ject to uncertainties until these triplet states can be observed and characterized.

Calcium oxide and strontium oxide suffer similar deficiencies.<sup>23,24</sup> Triplet states have not been assigned in BeO, MgO, CaO, SrO or BaO. Absorption from a  $^3\Pi$  has been reported<sup>25</sup> for BeS indicating low-lying triplets in this molecule.

The search for triplets has been complicated by the stability of alkaline earth hydroxides. Experimentally the removal of traces of water in a high-temperature spectral source has proven difficult. Deuterium isotope work<sup>14,16</sup> has shown that some observed features of the MgO violet spectrum can be attributed to MgOH. The existence of molecules such as  $Mg_2O_2$  has been suggested.<sup>2,14</sup>

Additional interest in the MgO spectrum was created by the reported spectroscopic constants of the  $C^1\Sigma^-$  and  $D^1\Delta$  electronic states.<sup>20</sup> Table I summarizes the data from the most recent papers on the violet system,<sup>20</sup> the green and the red systems.<sup>6</sup> The nearly identical spectroscopic constants raise the possibility that the  $C^1\Sigma^-$  and  $D^1\Delta$  are not singlets at all but  $\Omega$  components of a triplet. Recent work on  $Se_2$ <sup>26</sup> indicates that the observed "singlets" are actually the Hund's case c)  $0^+ - 0^+$  and 1-1 transitions of the Hund's case a)  $^3\Sigma^- - ^3\Sigma^-$  transition.

In light of recent progress in high resolution analysis it seemed reasonable to re-examine the complex violet system in medium resolution. The spectroscopic constants of the three states involved in the known violet transitions allow the calculation, in principle, of all features due to these electronic states. Any additional features may be due to other electronic transitions, other magnesium molecular species or other

Table I.

Spectroscopic constants for known magnesium oxide electronic states (K)

Constant	$X^1\Sigma^+$	$A^1\Pi$	$B^1\Sigma^+$	$C^1\Sigma^-$	$D^1\Delta$
$T_e$	0.0	3563.27	19 983.95	30 080.55	29 851.63
$\omega_e$	785.06	664.44	824.08	632.5	632.4
$\omega_e \times e$	5.18	3.91	4.76	5.3	5.2
$B_e$	.5743	.5050	.5822	.5014	.5008
$\alpha_e$	.0050	.0040	.0045	.0048	.0048
$D_e \times 10^6$	1.22	1.165	1.14	1.245	1.255
$\beta_e \times 10^8$	2.0	1.0	2.5	3.0	3.0
$H_e \times 10^{12}$	0.0	5.9	0.0	5.0	4.8

$\Omega$  triplet components if the C-A and D-A transitions are portions of a triplet-singlet or triplet-triplet transition.

The ultra-violet spectral region from about 2800 Å to 3300 Å as well as other regions throughout the ultra-violet and visible regions have strong OH transitions.<sup>27</sup> In any arc system which uses  $O_2$  this contaminant is particularly difficult to remove. In view of the large number of expected MgO transitions extra effort to remove this impurity might well reveal an unanalyzed electronic transition of MgO which could yield information about the unobserved triplet states.

## II. THEORETICAL PREDICTIONS

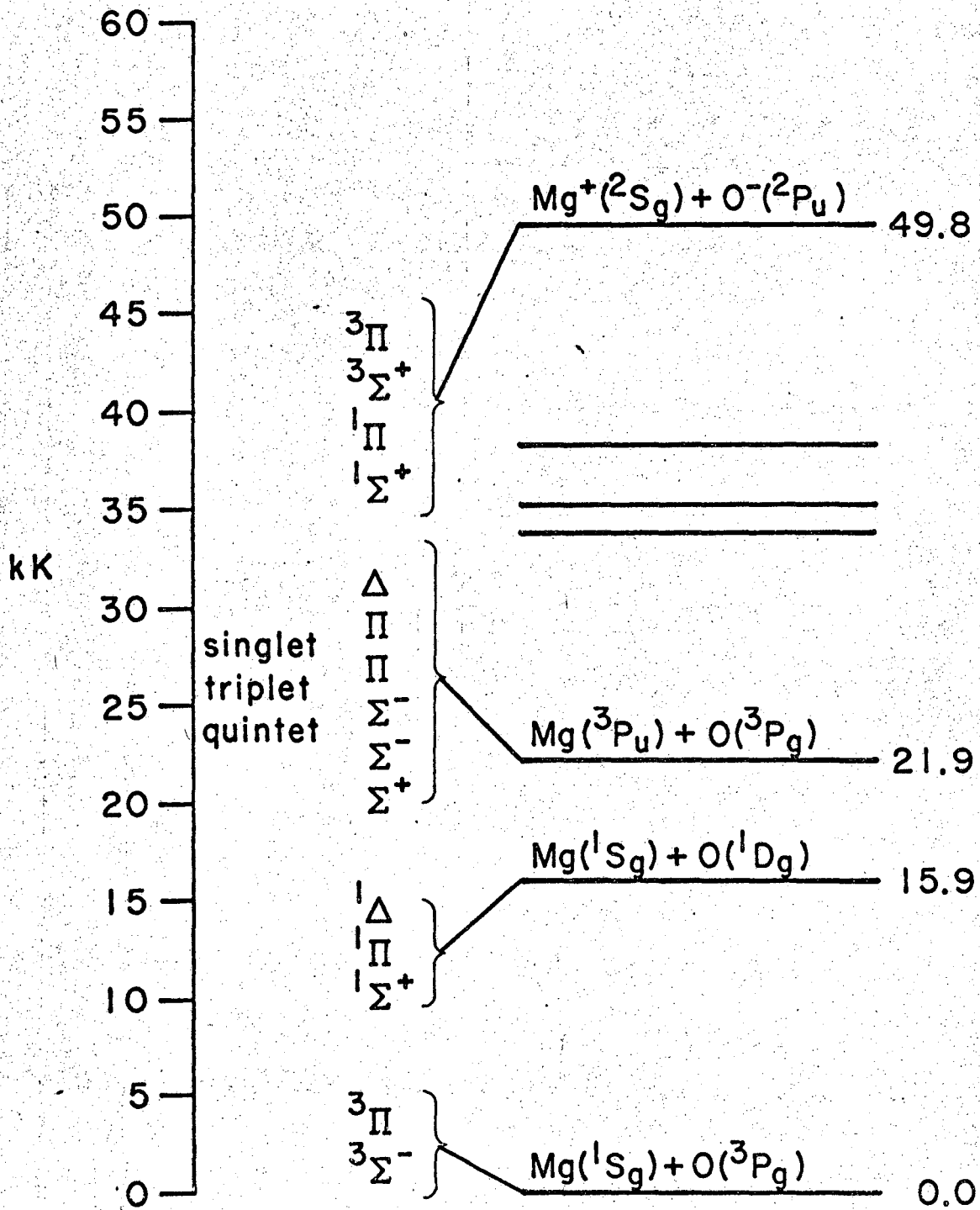
### A. Expected Electronic States

One of the most striking results of a consideration of the molecular states arising from various atomic states of magnesium and oxygen is that only triplet molecular states arise from ground state atoms. Figure 2 shows the molecular states of MgO from low-lying atomic states. The atomic energies have been taken from Moore.<sup>28</sup> The lowest atomic configuration which gives singlet electronic molecular states is 15.9 kK ( $15,900 \text{ cm}^{-1}$ ) above the ground state atoms. A singlet molecular ground state from neutral atoms would be expected only if the bonding energy between magnesium  $^1\text{S}$  and oxygen  $^1\text{D}$  is at least 15.9 kK larger than the bonding between magnesium  $^1\text{S}$  and oxygen  $^3\text{P}$ .

The number of molecular states arising from the magnesium  $^3\text{P}$  with the oxygen  $^3\text{P}$  is very large. Some or even most of these states might be repulsive. In general, the wealth of molecular electronic states arising from low-lying atomic states suggest the possibility of a large number of perturbations and predissociations as well as many allowed electronic transitions.

Using an ionization potential of 7.64 e.v. for magnesium<sup>28</sup> and an electron affinity of 1.47 e.v. for oxygen<sup>29</sup> (1 e.v. = 8.067 kK), the ground state ions lie about 49.8 kK above the ground state of the neutral atoms. This is low enough to have a considerable effect on the character of the low-lying electronic states if it does not in fact give rise to the molecular ground state.

Herzberg<sup>30</sup> has suggested the following empirical rule. If  $r_s$ , the internuclear distance at which the Coulomb attraction energy is equal to



XBL 682-122

Fig. 2 Magnesium oxide electronic states arising from atomic energy levels.

the difference between the ionic ground state energy and the neutral atomic ground state energy, is greater than twice  $r_e$ , the equilibrium internuclear distance of the molecular ground state, then the ground state is ionic in character. In other words, an ionic ground state will occur when the Coulomb potential curve can "cross" the potential curve of neutral atoms at a distance where the neutral curve is nearly at the dissociation energy. If  $r_s$  is less than 1.5 times  $r_e$ , the curves will not cross. This rule seems to have validity when applied to some nine-valence-electron diatomic molecules<sup>31</sup> including the alkaline-earth monohalides.

The value of  $r_s$  is approximately 4.1 Å for MgO which exceeds the  $r_e$  of the  $X^1\Sigma^+$  (1.749 Å)<sup>6</sup> by over a factor of two. This suggests that the ionic states  $1\Sigma^+$ ,  $1\Pi$ ,  $3\Sigma^+$  and  $3\Pi$  will be of considerable importance to the spectrum of MgO and to the thermodynamic partition function. It is possible that one of these ionic states is the molecular electronic ground state.

Brewer<sup>21</sup> has compared the electronic energy levels of several eight-valence-electron molecules including MgO. The basis of comparison is systematic trends of the relative energies of different molecular orbitals as the nuclear charge is changed. Table II reproduces his compilation and predictions. The lack of data for the alkaline earth oxides is apparent. The homonuclear molecule  $C_2$ , which has been well studied, has six electronic states with an observed  $T_e$  value of 20 kK or less and two additional states are predicted within this energy range. Only three states have been observed for MgO with an energy of 20 kK or less. The selection rules are less stringent for MgO than for  $C_2$  which has additional symmetry requirements on allowed transitions.<sup>30</sup> States which are inaccessible from the ground state in  $C_2$  could be seen in MgO.

Table II.

Energies of electronic levels of some eight-electron molecules in kK.<sup>21</sup>

Molecular Orbital Configuration	Electronic State	Observed or Predicted			Electronic Energy kK	
		C <sub>2</sub>	BeO	MgO	CaO	SrO
$\sigma^2 \sigma \pi^4 \sigma$	$1\Sigma^+$	43.2	(35±5)	(30)	28.8	28.5
	$3\Sigma^+$	13.3	(20±7)	(20±5)	(18±5)	(18±5)
$\sigma^2 \sigma^2 \pi^3 \sigma^2$	$1\Pi$	34.3	(30±5)	(28±4)	25.9	24.0
	$3\Pi$	20.0	(20±5)	(20±10)	(19±5)	(18±5)
$\sigma^2 \sigma^2 \pi^2 \sigma^2$	$1\Sigma^+$	(20±2)	21.3	20.0	11.5	10.9
	$1\Delta$	(13±5)	(14±5)	(15±5)	(8±5)	(6±2)
	$3\Sigma^-$	6.4	(7±3)	(8±5)	(3±5)	(1±1)
$\sigma^2 \sigma^2 \pi^3 \sigma$	$1\Pi$	8.4	9.4	3.6	(3±2)	(2±1)
	$3\Pi$	0.7	(1±1)	(-1±2)	(-1±2)	(-1±1)
$\sigma^2 \sigma^2 \pi^4$	$1\Sigma^+$	0	0	0	0	0

It should be pointed out that comparisons based on the molecular orbitals of the valence molecular orbitals are valid only when correlation energies are comparable or varying smoothly with nuclear charge. It would be expected that the alkaline-earth oxides should show trends. These trends should be useful in predicting unobserved electronic states' energies. The use of  $C_2$  as a basis for the prediction of energy levels of MgO requires care. The correlation energy may be estimated from atomic correlation energies by doing population analyses of the molecular orbitals. The population analysis is a computation of the probability density of an electron in a given molecular orbital relative to the two atomic configurations. For the molecular orbitals involved in comparing  $C_2$  to MgO, the population analysis will be quite different due in part to the ionic character of MgO. In order to satisfactorily predict the electronic energies of MgO from those of  $C_2$ , account must be taken of these differences.

Ab initio ICAO MO SCF calculations have been performed<sup>22</sup> for three molecular orbital configurations of MgO. Table III summarizes the results obtained for the molecular electronic term values including a semi-empirical correlation energy correction. It should be noted that before application of this correction term, both the  $^3\Pi$  and  $^3\Sigma^+$  states were lower in energy than the  $^1\Sigma^+$  state by about 12 and 9 kK respectively. The uncertainties involved in proper application of the correlation energy correction term make the final term energies uncertain to such a degree that the identity of the ground state is not conclusive. It should also be pointed out that these authors' conclusion that the experimental failure to observe triplets is not surprising, is valid if no other triplet states are within about 40 kK of the ground state. Their conclusion is apparently based on the



Table III. Low-lying molecular orbitals of magnesium oxide

Molecular Orbital Configuration	Electronic State	Calculated Energy (kK) <sup>22</sup>
$1\sigma^2 2\sigma^2 3\sigma^2 1\pi^4 4\sigma^2 5\sigma^2 2\pi^4 6\sigma^2$	$1\Sigma^+$	0.0
$2\pi^3 6\sigma^2 7\sigma$	$3\Pi$	2.3
	$1\Pi$	4.6
$2\pi^4 6\sigma 7\sigma$	$3\Sigma^+$	2.3
	$1\Sigma^+$	12.8
$2\pi^2 6\sigma^2 7\sigma^2$	$3\Sigma^-$	
	$1\Delta$	
	$1\Sigma^+$	
$2\pi^3 6\sigma 7\sigma^2$	$3\Pi$	
	$1\Pi$	
$2\pi^4 7\sigma^2$	$1\Sigma^+$	

calculated near degeneracy of the two triplet states arising from the three molecular orbital configurations they considered. Table 3 lists other molecular orbital configurations and the resultant molecular electronic states which might be expected to be important to the electronic spectrum within the photographic limits. All these states arise from different populations of the same molecular orbitals which were considered in the calculations. Rough estimates of their energies may be obtained from the calculated term energies. It would seem surprising if there were not at least two other triplet states,  $^3\Sigma^-$  and  $^3\Pi$ , below 40 kK. It should be noted that none of the molecular orbitals considered give a  $^1\Sigma^-$  state.

The energies obtained by calculations of this type for the separation of electronic states of the same molecular orbital configuration are more accurate, in general, than the difference in energies of different molecular orbital configurations. If the lowest calculated  $^1\Sigma^+$  and  $^1\Pi$  correspond to the two lowest observed states of MgO (see Fig. 1), then from the  $^3\Pi-^1\Pi$  separation of Table III, the  $^3\Pi$  should be less than 1 kK above the  $X^1\Sigma^+$ . This is of extreme thermodynamic importance since the contribution of the  $^3\Pi$  state to the electronic partition function is a factor of six whereas it is only one for the  $^1\Sigma^+$ .

A recent molecular calculation determined the  $^3\Pi-^1\Pi$  separation of BeO to be less than 1 kK.<sup>32</sup> The authors suggest that the comparable splitting should be even less in MgO.

The linear Birge-Sponer extrapolation is often an effective method for estimating molecular dissociation energies. It generally tends to give slightly large dissociation energies.<sup>33</sup> If the molecular vibrational energy levels may be reasonably represented by Eq. (1), then the convergence of

Table IV.

Dissociation energies of observed magnesium oxide electronic states.

State	$D_e$ (kK)	$T_e$ (kK)	Total Energy (kK)
$X^1\Sigma^+$	29.7	0.0	29.7
$A^1\Pi$	28.3	3.6	31.9
$B^1\Sigma^+$	35.7	20.0	55.7
$C^1\Sigma^-$	19.2	30.1	49.3
$D^1\Delta$	18.9	29.9	48.8

/ has the largest  $D_e$  value and is the only state with a total energy (relative to the  $X^1\Sigma^+$ ) greater than the difference between ground state neutral atoms and ground state ions. The energy difference between the 30 kK limit of the  $X^1\Sigma^+$  and  $A^1\Pi$  states and the 49 kK limit of the  $C^1\Sigma^-$  and  $D^1\Delta$  is near the 15.9 kK energy difference which was sought. Because of inherent inaccuracies of this method of calculation of  $D_e$  it is not safe to draw any conclusions from Table IV. However, any proposed scheme of dissociation products must be consistent with the data contained in that table.

In summary, low-lying triplet molecular states for MgO are extremely probable and the ground state could be either a singlet or a triplet based on theoretical considerations. The relatively low-lying singly charged atomic ionic states lead to the likelihood that the ground state is ionic in character. No unambiguous calculations or predictions are available concerning the nature of the molecular electronic ground state.

these levels represents the dissociation limit given by Eq. (2).

$$G(v) = \omega_e (v + 1/2) - \omega_e x_e (v + 1/2)^2 \quad (1)$$

$$D_e = \frac{\omega_e^2}{4 \omega_e x_e} \quad (2)$$

The Morse potential function<sup>34</sup> given by Eq. (3), when put in the molecular Schrodinger equation gives a formula for the vibrational energy levels which is equivalent to Eq. (1). Thus, Eq. (2) represents the dissociation limit of a Morse potential.

$$V(r) = D_e [1 - \exp [-a (r - r_e)]]^2 \quad (3)$$

Although many analytical functions have been suggested to represent the potential curve of molecular vibration,<sup>35</sup> the Morse potential has sufficient accuracy for many purposes without undue mathematical complications. It does often give a reasonable estimate of the dissociation limit.

Care must be taken in applying Eq. (3) to states which may be ionic in character. It has been shown<sup>33</sup> that this simple formula is valid only when the force of molecular attraction is proportional to a power of  $(1/r)$  greater than four. Clearly a Coulomb attraction,  $(1/r)^2$ , is not represented well by Eq. (3).

Equation (3) was applied to all known states of MgO using the constants of Table I without regard to possible limitations imposed by expected ionic character. The purpose was primarily to see if the 15.9 kK energy difference between the atomic states which give rise to molecular triplet states and those atomic states which give rise solely to molecular singlet states (see Fig. 2) could be observed. Table IV summarizes the results. The  $B^1\Sigma^+$  state

### B. Computer Program

Program "Heads" was written to predict the wavelength of band heads belonging to transitions between known electronic states. The program is explained in detail in Appendix A.

The complex violet system of MgO-MgOH has two assigned transitions, the  $C^1\Sigma^- - A^1\Pi$  and the  $D^1\Delta - A^1\Pi$  of MgO. Only the (0,0) and (1,1) vibrational bands of each transition have been rotationally analyzed.<sup>19,20</sup> In order to properly assign other band heads in the spectral region 3600-4000 Å, accurate calculations were needed for the wavelengths of other vibrational bands of these known electronic transitions.

The rotational energy of MgO requires three terms in the expansion of  $J(J + 1)$  in order to adequately represent the observed rotational energy levels at high  $J$ .<sup>20</sup> Many band heads of the violet systems occur at high  $J$  due to the similarity of  $B_v'$  and  $B_v''$ . Program "Heads" solves the third order polynomial for the  $J$  of the head. The results have given the desired accuracy. However, the linear equation for the  $J$  of the head (i.e., neglect of  $D_v$  terms) gave erroneous results for the wavelength. In some cases, the linear equation even gave a head in the wrong branch.

Because of the large density of band heads in the violet spectral region, accuracy is essential in order to unambiguously assign observed band heads. Results of the application of program "Heads" to the violet systems of MgO will be presented with the experimental results.

It should be mentioned that program "Heads" is particularly applicable to molecules where accuracy is required and the band heads occur at high  $J$ .

### III. EXPERIMENTAL

#### A. Spectrographs and Photographic Materials

The principle spectrograph used in this work was a 0.75 meter Spex. It has a Czerny-Turner kinematic mount for interchangeable gratings. A one micron blaze grating with 600 lines/mm was used in third order for study of the violet band systems. The resultant reciprocal linear dispersion was about  $7.1 \text{ \AA/mm}$  and with a ten micron slit width, the resolution was  $.07 \text{ \AA}$ . For the ultra-violet region at wavelengths shorter than  $3000 \text{ \AA}$ , a  $5000 \text{ \AA}$  blaze grating with 1200 lines/mm was used in second order. The reciprocal linear dispersion was about  $5 \text{ \AA/mm}$  corresponding to a resolution of  $0.05 \text{ \AA}$ . This same grating was used in first order for study of both the red and green systems of MgO. The instrument aperture is  $f/6.8$ .

Kodak 103 a-0 photographic plates were used to photograph the spectral region from  $2500\text{-}4500 \text{ \AA}$  and Kodak 103 a-F plates were used from  $4500\text{-}6500 \text{ \AA}$ . The standard development procedure was four minutes in Kodak D-19 developer; ten seconds in acid stop; five minutes in Kodak Rapid Fixer and thirty minutes in a water wash bath all at  $20^\circ\text{C}$ .

A Steinheil prism instrument was used in part of the work in a Raman spectral arrangement. The collimator focal length was 195 millimeter and the camera focal length was 255 millimeter. The instrument aperture is  $f/4$ . Both a three-glass-prism and a two-quartz-prism arrangement were employed. The reciprocal linear dispersion varies considerably with wavelength and with the prism arrangement. With the three-glass-prism arrangement, the reciprocal dispersion varied from about  $10 \text{ \AA/mm}$  in the violet to over  $100 \text{ \AA/mm}$  in the red. The dispersion for the two-quartz-prism arrangement was smaller.

Kodak 103 a-F 35 mm film was used in a curved-focal plane holder to allow simultaneous focus of all wavelengths. The spectral sensitivity of this film varies within a factor of about three over the wavelength range of interest. Development procedures were identical to those for the photographic plates.

### B. Magnesium Oxide Vacuum Arc

The primary experimental problem is the elimination of traces of water from the system. A vacuum arc was designed to produce the MgO spectrum while minimizing OH and MgOH spectral impurities. Figure 3 shows a schematic diagram of the entire arc system including the arc power supply.

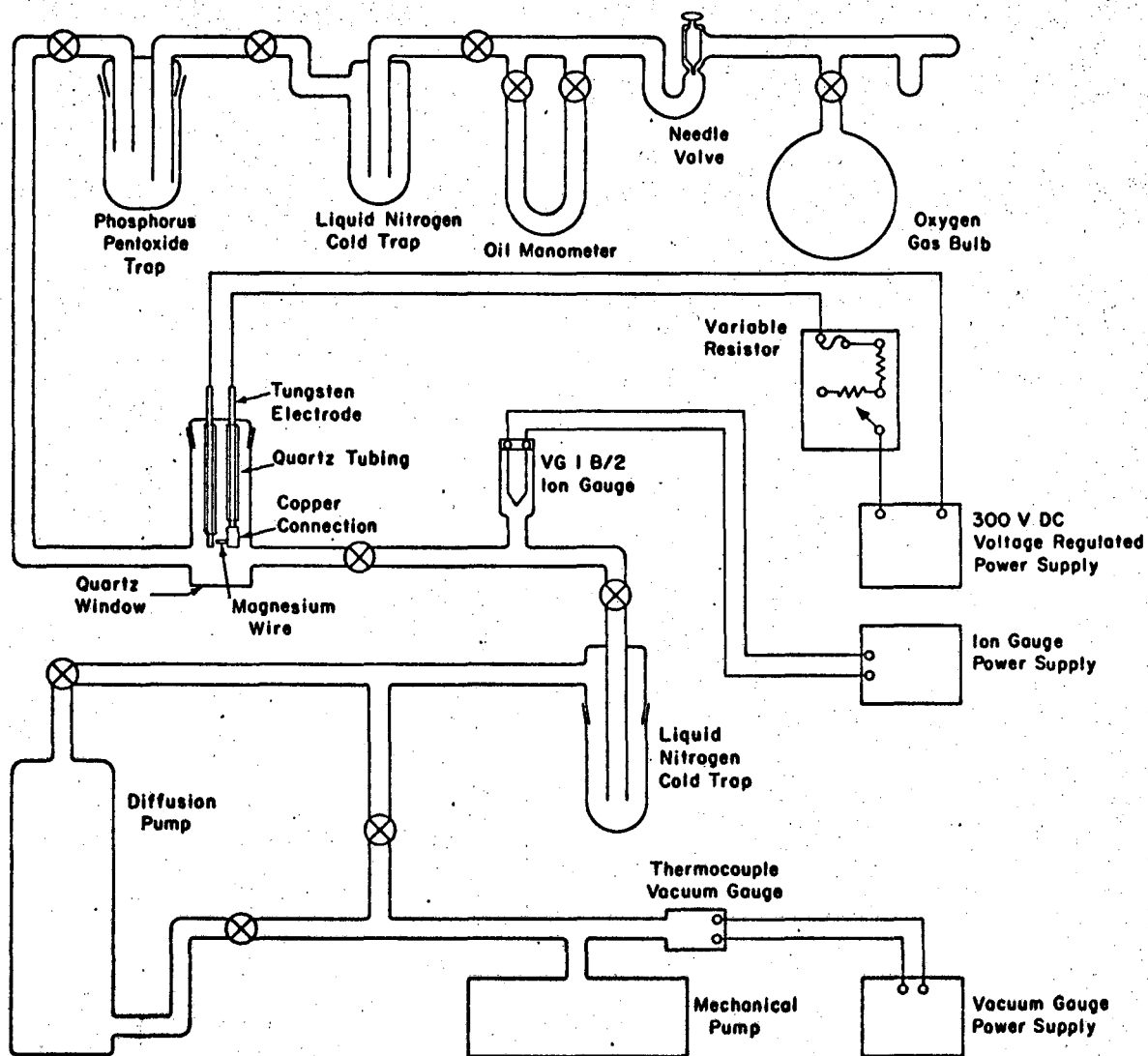
The arc electrodes were tungsten rods passed through pyrex with Kovar seals. A ground glass seal allowed easy removal of the electrodes for replacement of the magnesium and cleaning. Two centimeters of copper tubing was fit onto the end of the cathode and four to twelve pieces of thirty mil magnesium wire were fit into the hole drilled in the copper. Both tungsten rods were shielded with quartz to prevent spurious arcing. This system allowed about ten total minutes of exposure under the operating conditions. Usually exposures were taken in about thirty second intervals to prevent over-heating of the anode. The pyrex surrounding the arc was cooled with an air flow.

A variable resistor was connected in series with a Kepco Labs voltage regulated 300 volt D.C. power supply. The resistance was adjusted so that from 1.0 to 1.5 amperes were drawn from the source. The arc was initiated with a Tesla coil.

Background pressures of  $6 \times 10^{-1}$  torr were obtained with a four inch oil diffusion pump. The entire glassware system was heated several times to remove adsorbed water.

A phosphorous pentoxide trap was placed between the oxygen supply bulb and the arc.  $P_2O_5$  is one of the better drying agents and the residual water vapor is only  $2 \times 10^{-5}$  mg/liter at  $25^\circ C$ .<sup>36</sup> Glass wool prevented the  $P_2O_5$





LBL 682-123

Fig. 3 Vacuum arc apparatus for producing the electronic spectrum of magnesium oxide.

from entering the area of the arc. A liquid nitrogen trap was also employed to condense out any water contaminant in the oxygen. The liquid nitrogen trap was placed between the oxygen supply and the  $P_2O_5$  trap to prevent the blowing of ice particles into the area of the arc. A needle valve was employed to control oxygen input into the arc. A silicon oil manometer measured the oxygen pressure and the typical pressure was about one torr.

The arc was run in a closed system to prevent unnecessary consumption of oxygen. The image of the arc was focused by a 12.5 centimeter focal length lens with a magnification of about three onto the spectrograph slit. In most spectral regions the characteristic green color of the arc was put on the slit and the blackbody cathode radiation was focused just off the slit. In the ultra-violet the arc was refocused with the filters removed between exposures since the point of arcing changes as the magnesium is consumed.

A Corning color glass filter 7-59 was used in violet spectral region to prevent second and fourth order lines from overlapping the third order band heads. The plate sensitivity removed first order features. A nickel sulphate-cobalt sulphate filter<sup>37</sup> was used below 3200 Å to attenuate visible light. Corning color glass filters 7-54, 0-53, 0-52 and 3-68 were used in the spectral regions 3000-3400 Å, 4000-5000 Å, 4500-6000 Å and 5500-6500 Å respectively to prevent overlapping of different order.

Hg/Cd, Rb and Ne Osram spectral lamps were used as standard line sources. In the ultra-violet a mercury germicidal lamp was powered with a microwave diathermy power supply to give lines below 3000 Å. Combinations of the lamps were used in spectral regions where the number of standard lines was small. In addition, magnesium line internal standards were used where available.

### C. Measurement of Plates

The photographic plates were measured with a William Gaertner and Co. comparator. All standard line wavelengths in air were taken from the M.I.T. Tables.<sup>38</sup> Program "Stand" which is described in Appendix B calculated a least-squares fit for the wavelength in terms of the measured comparator distance using the known wavelengths. This polynomial was then applied to the comparator measurements of the unknown spectral features.

Both wavelengths in air and wavenumbers (K) in vacuum are reported. The formula of Edlen<sup>39</sup> was used with an additional correction term of  $1 \times 10^{-5}$  in the refractive index of air as an estimate of the maximum water vapor correction. The errors in the estimated correction factor effect the reported wavelengths less than experimental measurement errors.

All numbers reported are an average of at least five independent measurements. Second order polynomial fits were used since the plate dispersion is nearly uniform. Higher order polynomials exceed the accuracy of the comparator measurements.

#### IV. RESULTS

##### A. $C^1\Sigma^- - A^1\Pi$ and $D^1\Delta - A^1\Pi$ Band Heads

Tables V and VI compare the results of the computer calculations and heads to those observed by Pesic,<sup>10</sup> Verhaeghe,<sup>12</sup> Barrow and Crawford,<sup>9</sup> Pesic and Gaydon<sup>14</sup> and the experimental measurements of this work. No previous workers attempted to assign the band heads. All heads are given as Qv'v" etc., and the J at which the P or R-heads occur is given. Figure 4 shows a densitometer tracing of the (0,0) sequence of both band systems.

The (0,0) sequence of the  $C^1\Sigma^- - A^1\Pi$  has been observed by all previous workers. This sequence overlaps the (0,0) sequence of the  $D^1\Delta - A^1\Pi$  near the R55 head. The  $^1\Delta - ^1\Pi$  sequence has had fewer reported heads. The agreement between the computer calculated band heads and those observed is always within 1.0 K and usually within 0.2 K. A noticeable exception is the R44 head of the  $^1\Sigma^- - ^1\Pi$ . The agreement of this work with that of Pesic suggests that either an unknown feature in the same region obscured the head or that the head is perturbed.

The assignment of the (0,1) sequence of the C-A band system is difficult due to overlap from some violet degraded features that do not appear to form a regular series of heads. No previous workers have reported heads that correspond to the calculated heads of this sequence. Special attention was directed toward the observation and measurement of this sequence, but all photographic plates taken in this work gave obscuring features in this wavelength region. Part of the problem is the similarity of  $B_e'$  and  $B_e''$  for this transition. The Franck-Condon factors of the (0,0) sequence are very much larger than those of the (0,1) sequence for the D-A transition<sup>40</sup> and by inference for the C-A transition also. Much greater

exposure times were required and overexposure of some features resulted in the obscuring of the weaker ones. Impurities that are present in only trace amounts give observable spectra with long exposure times. Only the Q-heads of the (0,1) sequence were observed because of the high J value of the head of the first few members of the sequence of R branches. Figure 5 shows the (0,1) sequence of the D-A transition.

No other sequences of either the C-A or D-A transitions were observed. The computer calculated band heads are included in Tables V and VI for other sequences which might have the same order of intensity as the (0,1) sequences. No heads are listed where the J of the head is larger than 100. Observation of this head is unlikely due to the high excitation required.

The average error of experimental observation and measurement is about 0.1 K for the strong features and is slightly greater for some weaker ones. An uncertainty of about 0.2 K should be attached to the leading members of each sequence.

Pesic<sup>10</sup> has reported band head measurements on the MgO<sup>18</sup> molecule. His failure to find correspondence of the observed heads in the O<sup>18</sup> with all those in O<sup>16</sup> was of interest. Often an isotope shift will place previously obscured features into spectral regions where observation is possible. Oxygen containing impurities are often shifted differently than the features of interest. Assignment of the observations of Pesic was important to the complete understanding of this spectral region.

Program "Heads" was adapted to calculate isotopic band heads for MgO. The effect of isotopic substitution on the spectroscopic constants of molecules is well-known.<sup>30</sup> Tables VII and VIII list the results of the computer calculated heads in comparison with the observations of Pesic for MgO<sup>18</sup>.

All assignments of weak features are tentative. The agreement of the first few members of the (0,0) sequences of the C-A and D-A transitions and the (0,1) sequence of the D-A transition is good. Attention should again be called to the R<sub>44</sub> head of the C-A transition. The difference between the calculated and observed heads is large as it was for the MgO<sup>16</sup> molecule. In general, the agreement between calculated and observed values is not as good for MgO<sup>18</sup> band heads as it is for MgO<sup>16</sup>.

Naturally occurring magnesium has three stable isotopes. Mg<sup>25</sup> and Mg<sup>26</sup> constitute little more than 10% each and might be expected to contribute weak features to the violet spectrum. Tables IX and X show the expected positions of these isotopic band heads as well as the calculated isotopic shift. No observed heads could be assigned to either of these isotopic species.

Table V.  $MgO^{16} 1\Sigma^- - 1\Pi$  band heads

Head	J	Calcu- lated Å	Calcu- lated K	Pesic	Verhaeghe	Barrow and Crawford	Pesic and Gaydon	This work
R00	77	3766.1	26 545.0	26 545.1	26 543	26 545.9	26 545.2	26 545.0
R11	68	71.8	504.7	505.0	502	505.1	505.0	505.1
Q00		72.4	500.8	501.3		500.9	501.3	500.6
Q11		77.3	466.2	465.7	459	466.0	465.8	465.8
R22	62	77.8	463.0	462.9	459	462.7	462.9	463.1
Q22		82.6	429.1	428.9		431.8	429.0	428.8
R33	56	84.0	419.4	418.2	415	419.9	418.2	418.6
Q33		88.3	389.2	388.4			388.4	388.8
R44	51	90.5	374.0	371.0	368	373.2	371.0	371.7
Q44		94.4	346.8					346.3
R55	47	97.4	326.3					
Q55		3800.9	301.8					
R66	43	04.6	276.5					
R66		07.8	254.2					
R10	47	3682.5	27 147.8					
Q10		85.9	122.8					
R21	43	88.9	100.6					
Q21		92.0	77.8					
R23	93	3867.9	25 846.4					
Q01		68.2	844.2					
Q12		72.3	817.4					817.5
R34	83	74.0	805.9					
Q23		76.7	788.1					787.3
R20	32	3602.4	27 751.3					
Q20		04.6	734.4					
R31	30	09.8	694.8					
Q31		11.8	679.0					
Q02		3967.8	25 195.4					
Q13		70.8	176.4					
Q24		74.3	154.8					

Table VI  $MgO^{16} \Delta-1 \Pi$  band heads.

Head	J	Calcu- lated Å	Calcu- lated K	Pesic	Verhaeghe	Barrow and Crawford	Pesic and Gaydon	This work
R00	83	3798.2	26 320.6	26 320	26 314	26 320.2	26 320.5	26 320.4
R11	74	3804.2	279.3	279.6	273	279.1	279.6	279.0
Q00		05.2	272.0	271.8		271.8	271.9	271.7
Q11		10.3	237.3	237.2	231	237.4	237.3	237.4
R22	66	10.4	236.5					
Q22		15.7	199.8	200.1		200.8	200.1	200.2
R33	60	16.9	192.0		186	195		192.0
Q33		21.6	159.5				160.3	160.1
R44	54	23.7	145.4		139	145		144.3
Q44		27.9	116.4					116.9
R55	50	30.8	96.6					
Q55		34.7	70.5					
R66	45	38.4	45.4					
Q66		41.9	21.8					
R01	49	3713.6	26 920.4					
Q10		17.3	893.9					
R21	45	20.2	872.7					
Q21		23.5	848.6					
Q01		3902.8	25 615.4	25 616.7	25 600		25 616.7	25 615.6
Q12		06.9	588.5	589.0		591	589.1	588.2
R34	89	08.0	581.4					
Q23		11.4	558.8	559.2	561		559.2	558.4
R45	80	14.6	538.4					
Q34		16.4	526.3	526.5	519		526.5	526.2
R56	72	21.4	494.1					
Q45		21.8	491.0	490.2	480		490.3	490.8
Q56		27.7	452.9			454		452.3
R67	65	28.4	448.2					
Q67		34.0	412.0					
R20	33	3632.3	27 522.9					
Q20		34.6	505.2					
R31	31	39.9	465.7					
Q31		42.0	449.3					
Q02		4004.2	24 966.6					
Q13		07.3	947.5					



Table VII  $\text{MgO}^{18}\text{O}^{16}$   $1_{\Sigma}^{-} - 1_{\Pi}$  band heads.

Head	J	Calculated Å	Calculated K	Pesic	Calculated Isotope Shift	Observed Isotope Shift
R00	78	3766.4	26 543.1	26 543.1	- 1.9	-2.0
R11	70	71.9	504.5	504.4	- .2	- .6
Q00		72.3	501.4	501.0	.6	- .3
Q11		77.1	468.1	468.5	1.9	3.2
R22	63	77.6	464.5	464.0	1.5	1.1
Q22		82.2	432.3	428.1	3.2	- .8
R33	57	83.5	422.8	421.1	3.4	2.9
Q33		87.6	394.1	392.4	4.9	4.0
R44	52	89.8	379.3	376.8	5.3	5.8
Q44		93.5	353.5		6.7	
R55	48	96.3	333.9		7.6	
Q55		99.7	310.5		8.7	
R10	48	3685.4	27 126.4		-21.4	
Q10		88.6	102.6		-20.2	
R21	44	91.5	81.3		-19.3	
Q21		94.5	59.6		-18.2	
R23	94	3864.8	25 867.3		20.9	
Q01		64.8	866.9	25 866.6	22.7	
Q12		68.7	840.8		23.4	
R34	84	70.6	828.6		22.7	
Q23		73.0	812.3		24.2	
R45	76	76.5	789.0		24.3	
R20	33	3607.7	27 710.3		-41.0	
Q20		9.8	694.1		-40.3	
R31	31	14.7	656.5		-38.3	
Q31		16.7	641.4		-37.6	
Q02		3960.9	25 239.6		44.2	
Q13		63.9	220.8		44.4	

Table VII.  $\text{MgO}^{18}\text{O}^{16}\text{O}^{16}\Delta\text{-}^1\Pi$  band heads.

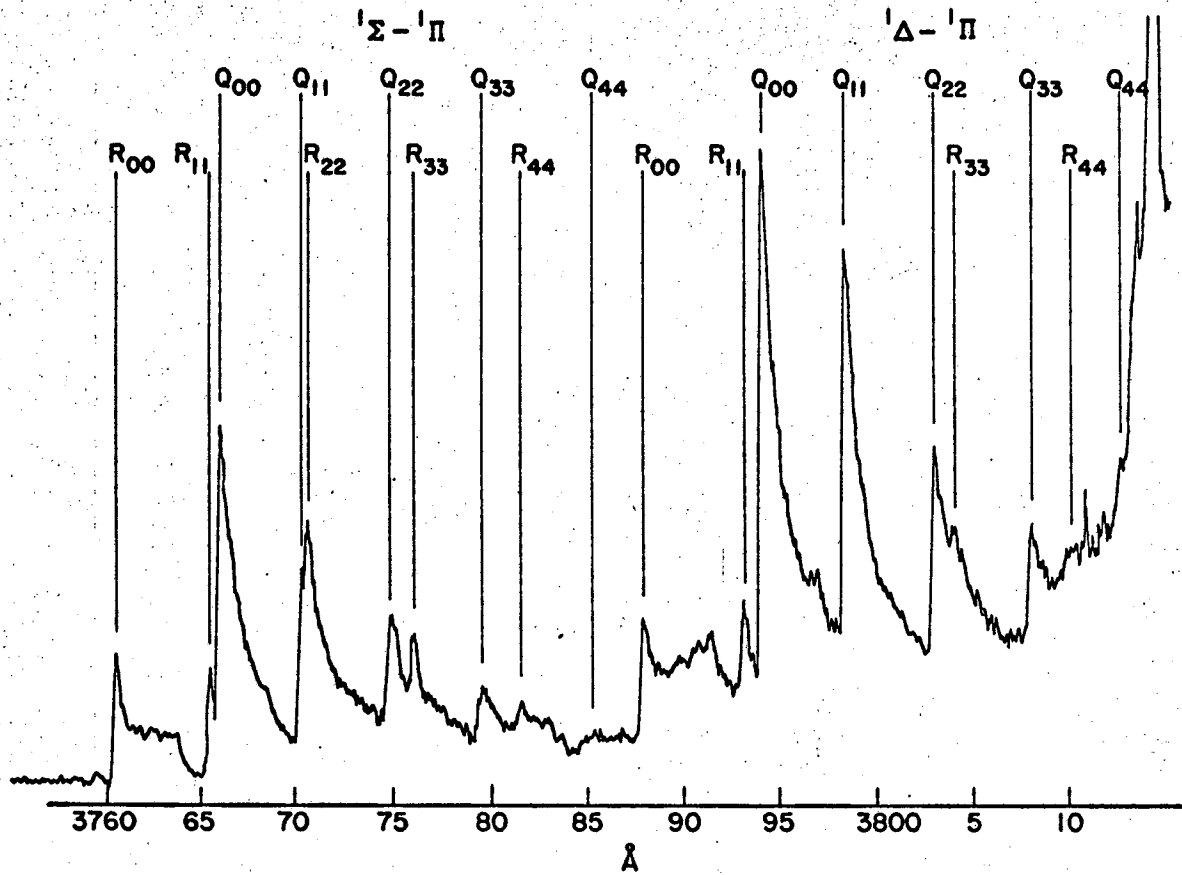
Head	J	Calculated Å	Calculated K	Pesic	Calculated Isotope Shift	Observed Isotope Shift
R00	85	3798.5	26 318.6	26 318	- 2.0	-2
R11	75	3804.2	278.9	278.1	- .4	-1.5
Q00		5.2	272.6	271.8	.6	0.0
Q11		10.0	239.2	238.1	.7	.9
R22	67	10.2	238.0	238.1	1.5	.9
Q22		15.3	203.1	202.0	3.3	1.9
R33	61	16.4	195.4	195.3	3.4	6.8
Q33		20.9	164.5		5.0	
R44	55	22.9	150.9		4.5	
Q44		26.9	123.2		6.8	
R55	51	29.7	104.3		7.7	
Q55		33.4	79.3		8.8	
R10	51	3716.5	899.0		-21.4	
Q10		20.0	873.7		-20.2	
R21	46	22.9	853.4		-19.3	
Q21		26.0	830.4		-18.2	
Q01		3899.3	25 638.1	25 638.3	22.7	21.6
Q12		3903.3	611.9	611.6	23.4	22.6
R34	91	4.5	603.9		22.5	
Q23		7.7	583.2	582.6	24.4	23.4
R45	81	10.8	562.7		24.3	
Q34		12.5	551.8	551.3	25.5	24.8
R56	73	17.3	520.3		26.2	
Q45		17.7	517.8	516.5	26.8	26.2
Q56		23.3	481.2		28.3	
R67	67	24.1	476.4		28.2	
R20	34	3637.7	27 481.8		-41.1	
Q20		40.0	465.0		-40.2	
R31	32	45.9	427.5		-38.2	
Q31		47.0	411.7		-37.6	
Q02		3997.1	25 010.8		44.2	
Q13		4000.2	24 991.9		44.4	

Table IX. Mg<sup>25</sup>O band heads.

Head	Upper State	J	Calculated Å	Calculated K	Calculated Isotope shift
R00	Δ	84	3798.3	26 320.1	- .5
R11	Δ	74	3804.2	279.2	- .1
Q00	Δ		5.2	272.2	.2
Q11	Δ		10.2	237.8	.5
R10	Δ	50	3714.3	915.4	-5.0
Q10	Δ		17.9	889.2	-4.7
Q01	Δ		3902.0	25 620.8	5.4
R20	Δ	34	3633.6	27 513.2	-9.7
Q20	Δ		35.9	495.7	-9.5
Q02	Δ		4002.5	24 977.1	10.5
R00	Σ	77	3766.2	26 544.5	- .5
R11	Σ	69	71.9	504.6	- .1
Q00	Σ		72.4	501.0	.2
Q11	Σ		77.3	466.7	.5
R10	Σ	47	3683.2	27 142.7	-5.1
Q10	Σ		86.5	118.1	-4.7
Q01	Σ		3867.4	25 849.6	5.4
R20	Σ	32	3603.7	27 741.6	9.7
Q20	Σ		5.8	724.9	9.5
Q02	Σ		3966.2	25 205.9	10.5

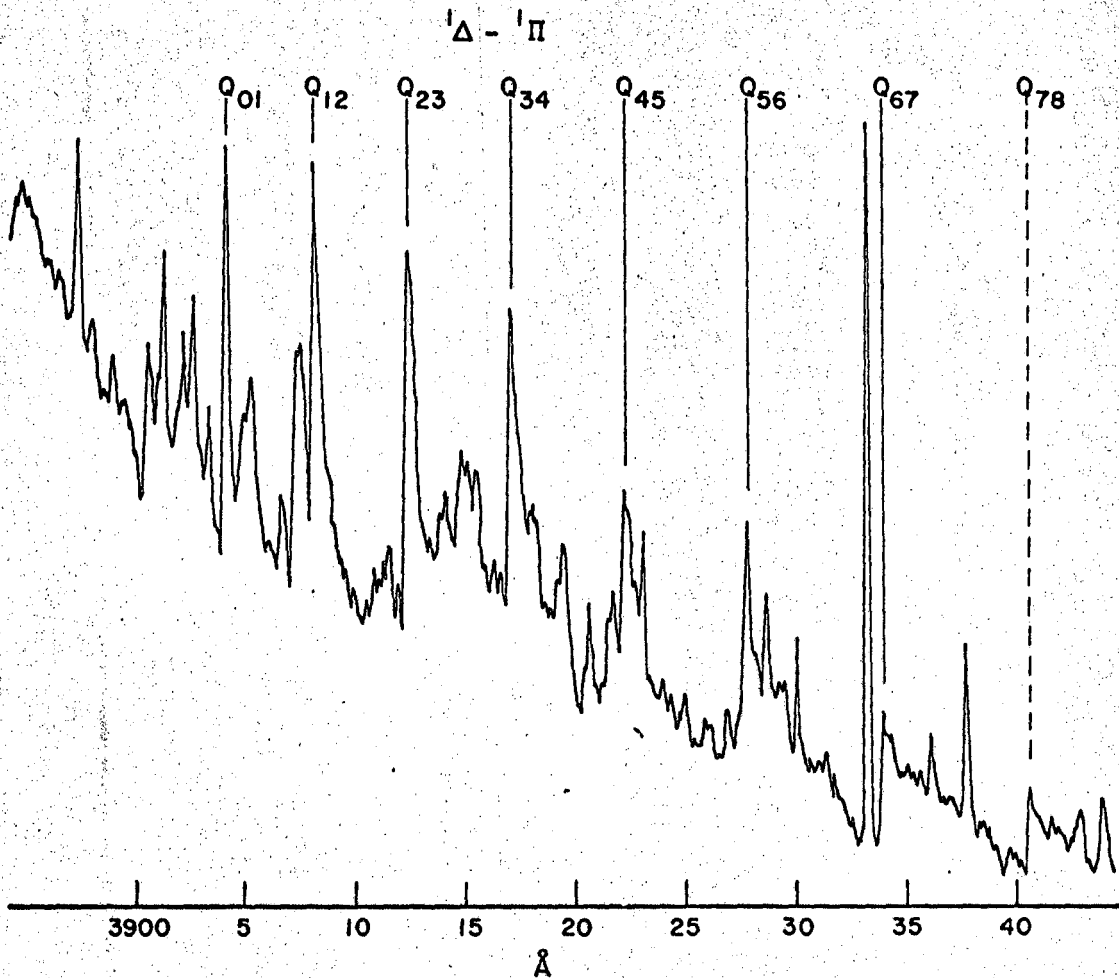
Table X.  $Mg^{26}O$  band heads.

Head	Upper State	J	Calculated $\lambda$	Calculated K	Calculated Isotope shift
R00	$\Delta$	84	3798.3	26 319.7	- .9
R11	$\Delta$	74	3804.2	279.1	- .2
Q00	$\Delta$		5.2	272.3	.3
Q11	$\Delta$		10.1	238.2	.9
R10	$\Delta$	50	3714.9	26 910.7	- 9.7
Q10	$\Delta$		18.5	884.7	- 9.2
Q01	$\Delta$		3901.2	25 625.8	10.4
R20	$\Delta$	34	3634.8	27 504.2	-18.7
Q20	$\Delta$		37.1	486.9	-18.3
Q02	$\Delta$		4001.0	24 986.8	20.2
R00	$\Sigma$	77	3766.2	26 544.1	- .9
R11	$\Sigma$	69	71.9	504.6	- .1
Q00	$\Sigma$		72.3	501.1	.3
Q11	$\Sigma$		75.9	476.1	.9
R10	$\Sigma$	47	3683.8	27 138.0	- 9.8
Q10	$\Sigma$		87.1	113.6	- 9.2
Q01	$\Sigma$		3866.7	25 854.6	10.4
R20	$\Sigma$	32	3604.8	27 732.6	-18.7
Q20	$\Sigma$		7.0	716.1	-18.3
Q02	$\Sigma$		3964.7	25 215.6	20.2



NBL 002-119

Fig. 4 Densitometer tracing of magnesium oxide  ${}^1\Sigma - {}^1\Pi$  and  ${}^1\Delta - {}^1\Pi$  (0,0) sequences.



XBL 682-120

Fig. 5 Densitometer tracing of magnesium oxide  ${}^1\Delta - {}^1\Pi$  (0,1) sequence.

### B. New Violet Band Systems

The band heads of sequences of the  $C^1\Sigma^- - A^1\Pi$  and  $D^1\Delta - A^1\Pi$  transitions have been calculated by program "Heads" with an accuracy exceeding 0.5 K in most cases. All expected isotopic band heads have also been calculated. It may be determined with reasonable certainty if any additional observed heads belong to the known electronic transitions.

There are a huge number of features in plates which over-expose the stronger features of this region. Some of these do not appear in all plates and are probably due to MgOH, OH or other contaminants. Some features in various plates have tentatively been attributed to CN, N<sub>2</sub> and perhaps CO. Not all weak features could be studied and only the apparent band sequences were measured.

The strongest band heads in this spectral region are the ones at 3720.6, 3721.0 and 3721.4 Å (see for example, ref. 27). These bands have an isotope shift in O<sup>18</sup> characteristic of a (0,0) sequence and the emitter is believed to contain only one oxygen atom.<sup>10</sup> These bands were observed but not measured in this work. These heads overlap the expected heads of the (1,0) sequence of the D-A transition.

Two other red-degraded band systems are apparent in this region. Table XI lists the measured heads of a band system previously observed by Pesic.<sup>10</sup> A densitometer tracing is shown in Fig. 6. Two additional members of this sequence have been observed in this work. The isotope shift in O<sup>18</sup> indicates that this is a (0,0) sequence. The heads are more closely spaced than the (0,0) sequences of the C-A and D-A transitions. The following formula represents the six observed band heads with an

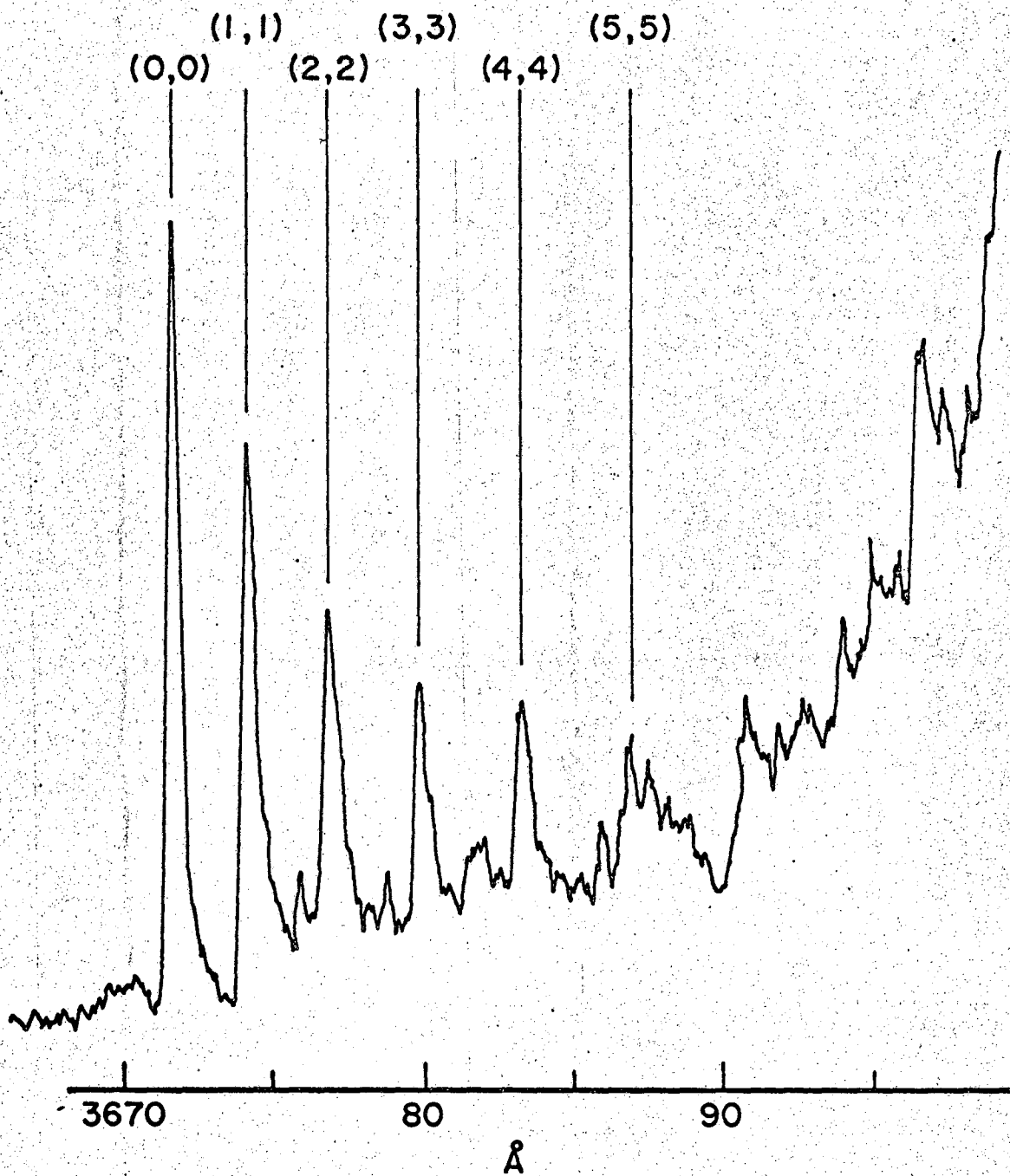
Table XI. New violet band system of  $\text{MgO}^{16}$ 

Band assignment ( $v', v''$ )	Observed wavelength	Observed wavenumbers (K)	Pesic observed (K)	Pesic isotope shift observed (K)
(0,0)	3672.1	27 224.4	27 224.5	-0.04
(1,1)	74.8	204.5	204.9	-0.12
(2,2)	77.7	182.9	183.3	-0.19
(3,3)	80.9	159.1	159.4	-0.28
(4,4)	84.4	133.1		
(5,5)	88.3	104.8		

Table XII. Weaker violet band system of  $\text{MgO}^{16}$ 

Wavelengths in air (Å)	Wavenumbers in vacuum (K)	Difference from previous head (K)
3637.3	27 484.5	
38.3	477.0	7.5
39.6	467.4	9.6
40.9	457.5	9.9
42.6	444.8	12.7
44.4	431.5	13.3
46.5	415.0	15.5





XBL 682-121

Fig. 6 Densitometer tracing of the (0,0) sequence of an unidentified transition in the magnesium oxide spectrum.

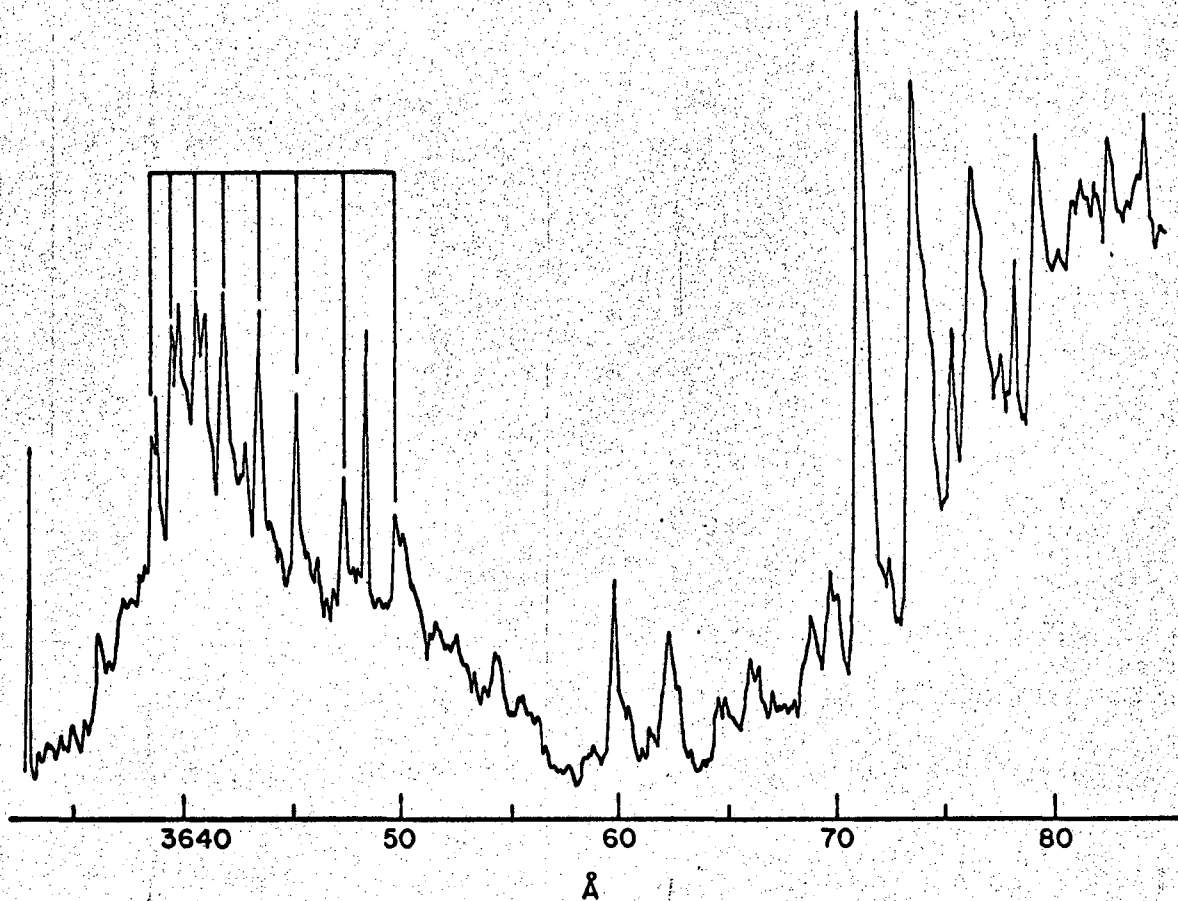
average error less than 0.1 K.

$$\nu = 27\,233.32 - 17.50 (\nu + 1/2) - 1.06 (\nu + 1/2)^2$$

If the heads are Q-heads of an MgO transition, then the intercept of the equation represents the difference in  $T_e$  values of the two states; the linear coefficient represents the difference in  $\omega_e$  values and the quadratic coefficient represents the difference in  $\omega_e x_e$  values. If the heads are R-heads of MgO, then the coefficients are approximate representations of these constants.

Some of the features between the heads in Fig. 6 may be due to the (1,0) sequence heads of the C-A transition. This severe overlap prevents the precise measurement of these weaker heads.

Table XII lists the heads of what may be an additional band system. Although agreement between observations of Pesic<sup>10</sup> and this work is not as good as for other band systems, it is clear that the same bands were observed. Several plates were taken to look at this band system. The intensity of these heads varied greatly relative to other features in this region. A densitometer tracing of a plate of this system is shown in Fig. 7 along with some of the heads of the previously mentioned unidentified (0,0) sequence. This plate was the only one where these two systems appeared to have comparable intensity. The first three heads are doubled due to overlap with an apparent violet degraded system which decreases rapidly in intensity at shorter wavelengths. These violet-degraded features appear to vary in intensity with the red-degraded ones from plate to plate. The doubled heads are included in Table XII because the spacing fits the undoubled heads although they may not be members of this sequence.



XBL 682-118

Fig. 7. Densitometer tracing of the weaker unidentified transition is the near-ultraviolet spectrum of magnesium oxide.

Pesic has observed an isotope shift in  $O^{18}$  which is characteristic of a (1,0) sequence of  $MgO^{10}$  for this band system. All of the heads, including the doubled ones, shift in a similar manner in  $O^{18}$ .

### C. Ultra-violet Band Systems

The number of expected electronic states below 50 kK implies the existence of a large number of allowed transitions. The upper state of one of the four analyzed band systems is not even predicted by consideration of the low-lying molecular orbitals. No triplet states have been assigned. For these reasons a systematic search of the MgO arc spectrum was undertaken to see if other band systems might be identified. Of particular interest was the region near 3000 Å which is obscured by strong OH bands.

The OH band heads at 3021.2, 3063.6, 3067.2 and 3089 Å were never entirely eliminated. They were substantially reduced in intensity by the addition of the P<sub>2</sub>O<sub>5</sub> trap to the system. Their open rotational structure partially obscured the entire region from 3021 Å up to about 3300 Å. No band systems other than OH were assigned in this region. If any MgO transitions lie in this region, their intensities must be substantially less than the intensities of the known red, green and violet transitions.

Some band heads were observed at shorter wavelengths which could not be attributed to OH or any other impurity listed in Rosen's Atlas<sup>41</sup> or in Pearse and Gaydon's compilation.<sup>27</sup> Table XIII lists these features. No sequence or progressions were observed among these bands and the nature of the emitter is uncertain.

The spectral region from about 2400 to 6500 Å was searched. No strong band heads other those listed in Table XIII and those attributable to known band systems were discovered.

Table XIII Unidentified features in the ultraviolet

Wavelength in air (A)	Wavenumbers in vacuum (K)	* Intensity	** Characteristic
2633.1	37 966.5	m	R
37.7	900.1	s	R
40.3	863.8	m	B
43.4	818.9	m	U
44.8	798.9	m	R
49.3	734.7	m	U
61.0	569.0	w	U
68.3	465.0	w	V
69.8	445.0	m	V
2749.2	36 363.4	w	V
50.2	350.2	s	V
51.6	331.0	m	V

\* Intensity: vw = very weak  
w = weak  
m = medium  
s = strong  
vs = very strong

\*\* Characteristic: R = red degraded band head  
V = violet degraded band head  
U = unidentified shading  
B = Broad, headless feature

#### D. Triplet Considerations

Consideration has been given to the possibility that one or more of the observed MgO transitions is a forbidden singlet-triplet transition. It would be expected that the f-value of such a transition would be at least a factor of  $10^2$  smaller than the f-value of an allowed transition. More likely it would be from  $10^4$  to  $10^6$  times smaller for a relatively light diatomic molecule such as MgO.

The violet, red and green band systems were photographed simultaneously on 103 a-F film using the Steinheil. Both the three glass prism Raman arrangement and the two quartz prism Raman arrangement were used.

Account was taken of the film spectral sensitivity, transmission of the glass prisms and the variation of dispersion with wavelength. Calculations show that the number of rotational lines within the resolving power of the spectrograph is large for the violet and green band systems where  $B_V'' \sim B_V'$ . For the red system  $B_V''$  and  $B_V'$  are substantially different so that the P-heads occur near the origin and the spacing of P lines increases rapidly away from the head. The red and green systems have a common upper state so their emission intensities are directly comparable. The violet upper states may have populations which are not easily comparable to the  $B^1\Sigma_g$ .

It may be qualitatively concluded that the four known band systems of MgO are of comparable intensity. The experimental results indicate  $f_{em}$ -values of the same order of magnitude.

The most unambiguous determination that two electronic transitions have a state in common is a comparison of the second differences. For a given vibrational level the second differences are identical for all

electronic transitions involving that state even if that state is perturbed by other electronic states.

$$\begin{aligned}\Delta_2 F''(J) &= R(J-1) - P(J+1) \\ \Delta_2 F'(J) &= R(J) - P(J)\end{aligned}\quad (4)$$

From the available experimental data, second differences were calculated for the lower state of the red system and the two violet systems ( $A^1\Pi$ ) for the  $v'' = 0$  and  $v'' = 1$  levels. Agreement was found among the three sets of second differences within experimental error. Theoretical second differences were calculated from known spectroscopic constants. For the  $A^1\Pi$  these theoretical values agree well with the experimentally determined ones.

The theoretical second differences for the  $C^1\Sigma^-$  and  $D^1\Delta$  were found to differ significantly from each other only at  $J$  values greater than about 65. This is just outside the range of observation. The second differences calculated from the experimental rotational lines are found to agree with each other within experimental error for the  $C^1\Sigma^-$  and  $D^1\Delta$ .

Because of the reported nature of the violet band systems, calculations were made to see when a triplet-triplet transition might appear to be a series of singlets. The reported strong Q-branches imply<sup>30</sup> a transition of  $\Delta\Lambda = \pm 1$ .

Intensity calculations were made using the formulas of Budo<sup>42</sup> for the twenty seven branches of a  $^3\Sigma^- \rightarrow ^3\Pi$  electronic transition. These Hönl-London formulas or line strengths give the intensity of a rotational line apart from the Franck-Condon factor, the Boltzmann factor and the electronic  $f$ -value. Relative branch intensities as a function of  $J$  were determined for



various degrees of coupling intermediate between Hund's cases a) and b).

For a  $^3\Pi$  in case a) the sublevel splittings between the  $\Omega = 2, 1$  and 0 components are both equal to A, the spin-orbit coupling constant.<sup>30</sup>

From the observed energy splitting between the C-A and D-A transition, the value of the hypothetical triplet A value is 228 K for the  $^3\Pi$  assuming the splitting to be negligible in the  $^3\Sigma$ .

The exact relative intensities are a function of J. The following qualitative conclusions were drawn for a J of about fifty. In the case b) limit, only the  $P_1, Q_1, R_1, P_2, Q_2, R_2, P_3, Q_3$  and  $R_3$  branches are of significant intensity. In this limit the A value is zero. In the case a) where A is large, twenty-seven branches have some intensity and twenty-four of them are within a factor of five at a J of fifty. Using the A value of 228 K and the  $B_0$  value of the  $A^1\Pi$  state, the case a) limit is closely approached.

The significance of these observations and calculations will be discussed later in this paper.

## V. CONCLUSIONS

### A. Violet Head Bands

Many of the previously unassigned band heads in the violet spectrum of magnesium oxide may now be considered assigned. All strong heads of the  $C^1\Sigma-A^1\Pi$  and  $D^1\Delta-A^1\Pi$  band systems have been calculated and observed. Some of the weaker heads have been observed and they also agree with the wavelengths calculated by program "Heads." This is experimental verification of the validity of the assumptions of the calculation and the accuracy of the reported spectroscopic constants of the states. It may be concluded that the other band heads of  $Mg^{24}O$ ,  $Mg^{25}O$ , and  $Mg^{26}O$  which were calculated but not observed are also accurate to better than 1.0 K for low vibrational quantum number.

These calculated heads will be of great value to further studies of this spectral region. The complexity of the spectrum may hinder observation of further heads attributable to any isotopic species of the C-A and D-A transitions. However, it may be easily determined if any new observed heads belong to these two transitions.

The  $v = 4$  level of either the  $^1\Sigma^-$  or  $^1\Pi$  may have a perturbation which causes the discrepancy between the observed and calculated band heads. No differences between the calculated and observed heads of this magnitude were found for the  $^1\Delta-^1\Pi$  so if a perturbation exists, it is probably in the  $^1\Sigma^-$ . Neither the (0,1) nor the (1,0) sequences of the C-A transition could be observed and measures so that no confirmation of the existence of a perturbation is possible. The measurements reported here and those of Pesic for this band head agree well. Since the intensity

is relatively weak in this head and the region is appreciably overlapped, it is unsafe to conclude that a perturbation does exist. Perhaps high resolution analysis of this band, if the exposure times required are feasible, would answer this question.

On the basis of qualitative observations of intensity variations from plate to plate and the general appearance of the spectrum, it is proposed that the emitter of the band system beginning at  $3672 \text{ \AA}$  is MgO. The bands have an appearance similar to the C-A and D-A transitions with a smaller spacing between heads. The series of six heads measured in this work form a sequence which fits the expected second order equation well. From Pestic's measured isotope shifts, the bands are a (0,0) sequence. High resolution analysis of this system could be of great value for further understanding of MgO electronic states.

The second band system observed in this work extending from  $3637$  to  $3647 \text{ \AA}$  is probably due to some emitter other than MgO. The very close spacing of heads is like the spectra of many polyatomic molecules. The irregular intensity variations of this system relative to other spectral features is indicative of an emitter other than MgO.

It seems likely that the strong features near  $3720 \text{ \AA}$  are due to MgO although the structure is unlike any known MgO band system. The substantial reduction of the OH heads near  $3000 \text{ \AA}$  suggests that impurities such as MgOH should appear only as weak features if at all. If the emitter of this system is MgO, then the upper and lower states must have nearly identical  $\omega_e$  values since there is no apparent development of a (0,0) sequence.

In view of the large number of weak unassigned features and the observed reduction of impurities in the arc, there may be other band systems in this region due to MgO. However, no sequences could be observed. All the strong features, with the exception of the bands mentioned, have been assigned.

In the entire spectral region from about 2400 to 6500 Å no strong sequences appear. The nature of the emitter or emitters of the unassigned bands around 2600 to 2800 Å is not clear. Perhaps very long exposure times might reveal additional heads which could be attributed to MgO, but it may be concluded from this work that there are no new strong heads due to MgO in the visible or near ultra-violet regions.

### B. Identification of Triplets

The  ${}^3\Pi$  and  ${}^3\Sigma^-$  molecular states arising from ground state magnesium and oxygen atoms should be low in energy unless they are both repulsive states. Ionic states are likely to be important in MgO including a  ${}^3\Sigma^+$  and a  ${}^3\Pi$  state. Molecular orbital considerations show a  ${}^3\Sigma^+$ ,  ${}^3\Sigma^-$  and two  ${}^3\Pi$  state. None of the molecular orbitals considered in this work give rise to a  ${}^1\Sigma^-$  state which might correspond to the C state of MgO. It may be concluded from these considerations that triplet states should be important to the MgO spectrum and that the existence of a  ${}^1\Sigma^-$  state at 30 kK is unexpected.

The curious problem of the nearly identical spectroscopic constants of the C and D states has not been resolved. Some clear statements may be made, however, concerning the possibility that these two states are triplet components rather than two singlet states.

It may be concluded that the C and D states are identical within experimental error. The second differences calculated in this work for these two states are not distinguishable within the range of experimental measurement. An alternative interpretation of the two MgO violet band systems, which is equally justifiable on the basis of reported experimental measurements, is that the upper states of the violet systems are common and the lower states are separated by 228 K.

It seems highly unlikely that the five known states of MgO are of different multiplicity. If the C and D states are triplet components, the the green and red band systems must be explainable also in terms of triplet states. The simultaneous observation of the violet, green and red band systems is quite strong evidence that all the reported electronic

transitions of MgO are allowed.

It may be concluded that the coupling of MgO is not intermediate between Hund's cases a) and b) if the violet system is to be explained as a  ${}^3\Sigma^- \rightarrow {}^3\Pi$  transition. The relative branch intensity calculations performed in this work indicates that too many branches should have appreciable intensity for the value of A obtained from the observed difference in energy of the two QOO band heads. In Hund's case c) the components of triplets are independent of one another and the spectroscopic constants are not necessarily similar as they are in case a). It would be expected on the basis of the relatively small molecular weight of MgO that case a) or case b) coupling should hold to a good approximation for the expected  ${}^3\Pi$  states.

It is difficult to accept the unprecedented observation of two indistinguishable singlet electronic states at nearly the same energy in a diatomic molecule. It is difficult to justify on the basis of molecular orbital theory the existence of a  ${}^1\Sigma^-$  state at the energy reported for the C state of MgO. Alternatively, if the C and D states are triplet components, then the green and red band systems should exhibit splittings similar to the violet system. No such splittings have been reported for these well-studied band systems.

This paradox can only be resolved by further examination of the MgO spectrum. Perhaps the analysis of an additional band system will answer some of the questions. Until the energies of the expected low-lying triplet electronic states can be experimentally determined, the spectral and thermodynamic properties of MgO will remain ambiguous.

REFERENCES

1. L. Brewer, Chem. Rev. 52, 48 (1953).
2. L. Brewer and R. F. Porter, J. Chem. Phys. 22, 1867 (1954).
3. E. M. Bulewicz and T. M. Sugden, Trans. Faraday Soc. 55, 720 (1959).
4. P. C. Mahanti, Phys. Rev. 42, 609 (1932).
5. P. C. Mahanti, Indian J. Phys. 9, 517 (1935).
6. A. Lagerqvist and U. Uhler, Arkiv För Fysik 1, 459 (1949).
7. A. Lagerqvist and U. Uhler, Nature 164, 665 (1949).
8. P. N. Ghosh, P. C. Mahanti and B. C. Makkerjee, Phys. Rev. 35, 1491 (1930).
9. R. F. Barrow and D. V. Crawford, Proc. Phys. Soc. A57, 12 (1945).
10. D. S. Pesic, Proc. Phys. Soc. A76, 844 (1960).
11. D. S. Pesic, Proc. Phys. Soc. A83, 885 (1964).
12. J. Verhaeghe, Wis-en Natuurk. Tijdsche 7, 224 (1935).
13. L. Brewer and S. Trajmer, J. Chem. Phys. 36, 1585 (1962).
14. D. S. Pesic and A. G. Gaydon, Proc. Phys. Soc. A73, 244 (1959).
15. D. S. Pesic and M. Kliska, Glasnik Hme. Drustva Beograd 28, 347 (1963),  
Chem. Abstract 63:3786A.
16. S. Trajmar, Ph.D. Thesis, University of California, Lawrence Radiation  
Laboratory Report, UCRL-9773 (July 1961).
17. S. Trajmar and G. E. Ewing, J. Chem. Phys. 40, 1170 (1964).
18. D. S. Pesic, Thesis for Doctorate, University of Belgrade (1961).
19. L. Brewer, S. Trajmar and R. Berg, Astrophys. J. 135, 955 (1962).
20. S. Trajmar and G. E. Ewing, Astrophys. J. 142, 77 (1965).
21. L. Brewer, Principles of High Temperature Chemistry in Proceedings of  
The Robert A. Welch Foundation Conferences on Chemical Research,

- (Robert A. Welch Foundation, Houston, Texas, 1962), pp. 47-92.
22. W. G. Richards, G. Verhaegen and C. M. Moser, *J. Chem. Phys.* 45, 3226 (1966).
  23. R. H. Hauge, Ph.D. Thesis, University of California, Lawrence Radiation Laboratory Report UCRL-16338 (October 1965).
  24. L. Brewer and R. Hauge, *J. Mol. Spect.* (in press).
  25. C. J. Cheetham, W. J. M. Gissane and R. F. Barrow, *Trans. Faraday Soc.* 61, 1308 (1965).
  26. R. F. Barrow, G. C. Chandler and C. B. Meyer, *Phil. Trans. Roy. Soc. London Aec. A.* 260, 395 (1966).
  27. R. W. B. Pearse and A. G. Gaydon, The Identification of Molecular Spectra, John Wiley and Sons, Inc., 3rd. Ed., New York (1963).
  28. C. E. Moore, Atomic Energy Levels, U.S. National Bureau of Standards, Circular No. 467 (1949).
  29. F. A. Elder, D. Villarejo and M. G. Inghram, *J. Chem. Phys.* 43, 758 (1965).
  30. G. Herzberg, Molecular Spectra and Molecular Structure, I. Spectra of Diatomic Molecules, D. Van Nostrand Co., Inc., Princeton, New Jersey (1950).
  31. M. D. Shetlar, Ph.D. Thesis, University of California, Lawrence Radiation Laboratory Report UCRL-11979 (April 1965).
  32. W. H. Huo, K. F. Freed and W. Klemperer, *J. Chem. Phys.* 46, 3556 (1967).
  33. A. G. Gaydon, Dissociation Energies, Chapman and Hall Ltd., 2nd Ed., London (1953).
  34. P. M. Morse, *Phys. Rev.* 34, 57 (1929).
  35. Y. P. Varshni, *Rev. Mod. Phys.* 29, 664 (1957).



36. A. Guthrie and R. K. Wakerling, Vacuum Equipment and Techniques, McGraw-Hill Book Co., Inc., New York (1949).
37. J. Strong, Modern Physical Laboratory Practice, Blackie and Son, Ltd., London (1938).
38. G. R. Harrison, Wavelength Tables, The Technology Press, M.I.T., John Wiley and Sons, Inc., New York (1938).
39. B. Edlen, J. Opt. Soc. Am. 43, 339 (1953).
40. Y. P. Srivastava and R. C. Maheshwari, Proc. Phys. Soc. 90, 117 (1967).
41. B. Rosen, Tables De Constantes et Donnees Numeriques, Atlas, Hermann Co., Paris (1952).
42. A. Budo, Zs. f. Phys. 105, 579 (1937).

## ACKNOWLEDGMENTS

I am grateful to Professor Leo Brewer who brought this problem to my attention and who has offered many helpful suggestions. His comprehensive knowledge of the chemical and spectroscopic problems related to this study has immensely aided the interpretation of results.

I appreciate the help of John Wang with the magnesium oxide arc apparatus. Thanks are due Nancy Monroe for the illustrations and Charlotte Machen and Pat Cookson for the typing of this manuscript.

I appreciate the encouragement and sacrifices of my wife, Sally.

This work was performed under the auspices of the United States Atomic Energy Commission.

## APPENDIX A

Program "Heads"

Program "Heads" was written for the CDC 6600 computer to calculate band heads from the spectroscopic rotational and vibrational constants. The program requires as input data  $\omega_e$ ,  $\omega_e x_e$ ,  $\omega_e y_e$ ,  $\alpha_e$ ,  $\alpha_e$ ,  $D_e$  and  $\beta_e$  for both electronic states as well as  $\Delta T_e$  for the transition. A flow diagram of the program is shown in Fig. 8. Table XIV lists the method of data input.

The vibrational energies and rotational constants for the initial vibrational level are calculated for both states.

$$G(v) = \omega_e(v + 1/2) - \omega_e x_e(v + 1/2)^2 + \omega_e y_e(v + 1/2)^3$$

$$B_v = B_e - \alpha_e(v + 1/2) \quad (5)$$

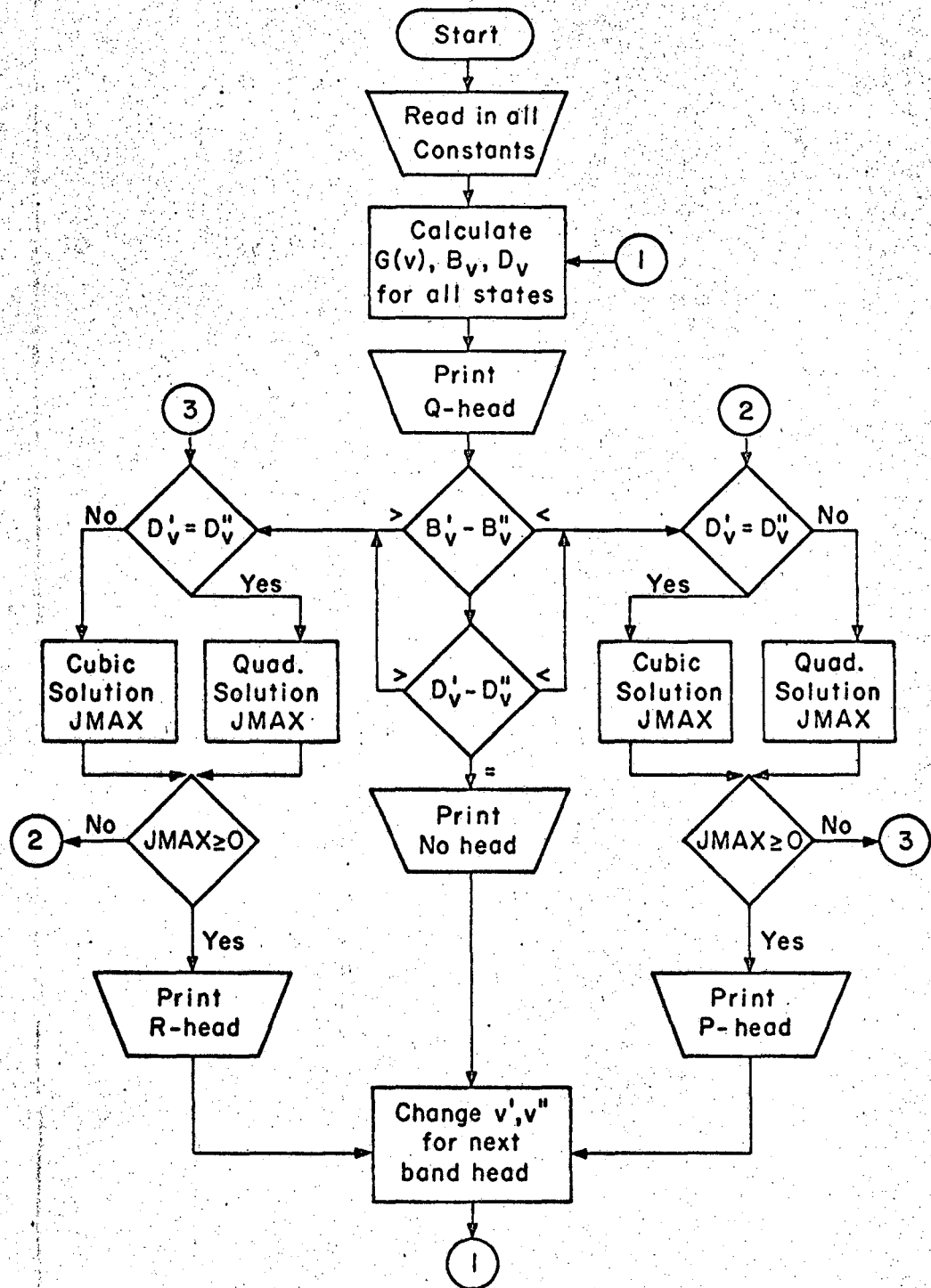
$$D_v = D_e + \beta_e(v + 1/2)$$

The Q-head occurs at the origin and may be calculated immediately. There is one Q-head for every band in this program. If the electronic transition is a  $\overset{1}{\Sigma} - \overset{1}{\Sigma}$  where Q-lines are forbidden, this part of the calculation may be omitted as explained in Table XIV.

$$\text{Origin} = \Delta T_e + G'(v) - G''(v) \quad (6)$$

The computer then calculates either a P or an R head for each band. Normally an R-head occurs when  $B_v'' > B_v'$  and a P-head when  $B_v'' < B_v'$ . If the  $B_v$  values are nearly identical in both states, the  $D_v$  values will determine the head.

The rotational energy,  $F_v(J)$ , of a vibronic state may be accurately expressed in terms of two constants. The neglect of higher terms could affect the J value and energy of calculated heads if J is large.



XBL 682-117

Fig. 8 Flow diagram of program "Heads".

$$F_v(J) = B_v J(J + 1) - D_v J^2(J + 1)^2 \quad (7)$$

R and P lines may be represented in terms of  $F_v(J)$ .

$$\begin{aligned} R(J) &= \text{Origin} + F_v'(J + 1) - F_v''(J) \\ P(J) &= \text{Origin} + F_v'(J - 1) - F_v''(J) \end{aligned} \quad (8)$$

The value of J at which a P-head is formed is found by solving the equation of  $P(J)/J = 0$ .

$$J^3 + J^2 \frac{3(D_v'' + D_v')}{2(D_v'' - D_v')} + J \frac{(B_v' - B_v'' - D_v' + D_v'')}{2(D_v'' - D_v')} - \frac{(B_v' + B_v'')}{4(D_v' - D_v'')} = 0 \quad (9)$$

If  $D_v'$  and  $D_v''$  are equal, the equation becomes quadratic and is treated separately in the computer. An analogous equation is solved for an R-head. Care must be taken to distinguish the physically real root or roots from the mathematical ones. It is physically possible to have reversal of shading. The computer will print three roots if the cubic roots for the J of the head are all real. Normally however, only one root is within the acceptable range of J values.

It should be noted that the  $D_v$  terms are very important in determining the heads in molecules like MgO. Estimates of the J of heads obtained by solving the linear equations (only  $B_v$  terms) are greatly in error. In addition, for some MgO bands the  $B_v$  values are so close that an R-head is formed even when  $B_v' > B_v''$ . This occurrence is handled, as shown in the flow diagram, by testing the J or the head (JMAX) to see if it is positive.

The vibrational limits of the upper and lower states are input data. The program normally begins with  $v' = 0$  and  $v'' = 0$  and increases  $v''$  by one

Table XIV Data input for program "Heads".

Section	Column	Datum	Definition	Format
1.	1-10	OEL	$\omega_e'$	F10.1
	1-10	OEXEL	$\omega_e^x'$	F10.1
	1-10	OYEL	$\omega_e^y'$	F10.1
	1-10	BEL	$B_e'$	F10.1
	1-10	AEL	$\alpha_e'$	F10.1
	1-10	DEL	$D_e'$	F10.1
	1-10	BEEEL	$\beta_e'$	F10.1
2.			Identical to sec. 1 with the spectroscopic constants of the lower state.	
3.	1-10	VOO	$\Delta T_e$ for the two electronic states.	F10.1
4.	1-10	VPMA	maximum $v'$	F10.1
	1-10	VPMI	minimum $v'$	F10.1
	1-10	VDMA	maximum $v''$	F10.1
	1-10	VDMI	minimum $v''$	F10.1
5.	1	KS	KS = 1 will skip Q-head calculation KS = 0 gives Q and either P or R heads	I1

until it reaches the chosen limit. Then it sets  $v' = 1$  and calculates the same number of band heads for this  $v'$ . It proceeds in this manner to the  $v'$  limit. Normally the band heads from (0,0) to (10,10) were calculated.

APPENDIX B

Program "Stand"

Program "Stand" gives wavelengths in Å in air and vacuum wave numbers in K for every measured line position. Lines of known position and wavelength are used as data points for a least-squares curve fitting. The polynomial obtained in this manner is applied to the observed positions to calculate their wavelengths.

If  $\overset{\circ}{A}_i$  signifies the wavelength in air and  $x_i$  the measured position of the  $i^{\text{th}}$  standard line, then the polynomial to be fitted is of the following form.

$$\overset{\circ}{A}_i = \sum_n^N c_n x_i^n \quad (10)$$

$N$  is the order of the polynomial and can be from one to nine in program "Stand."

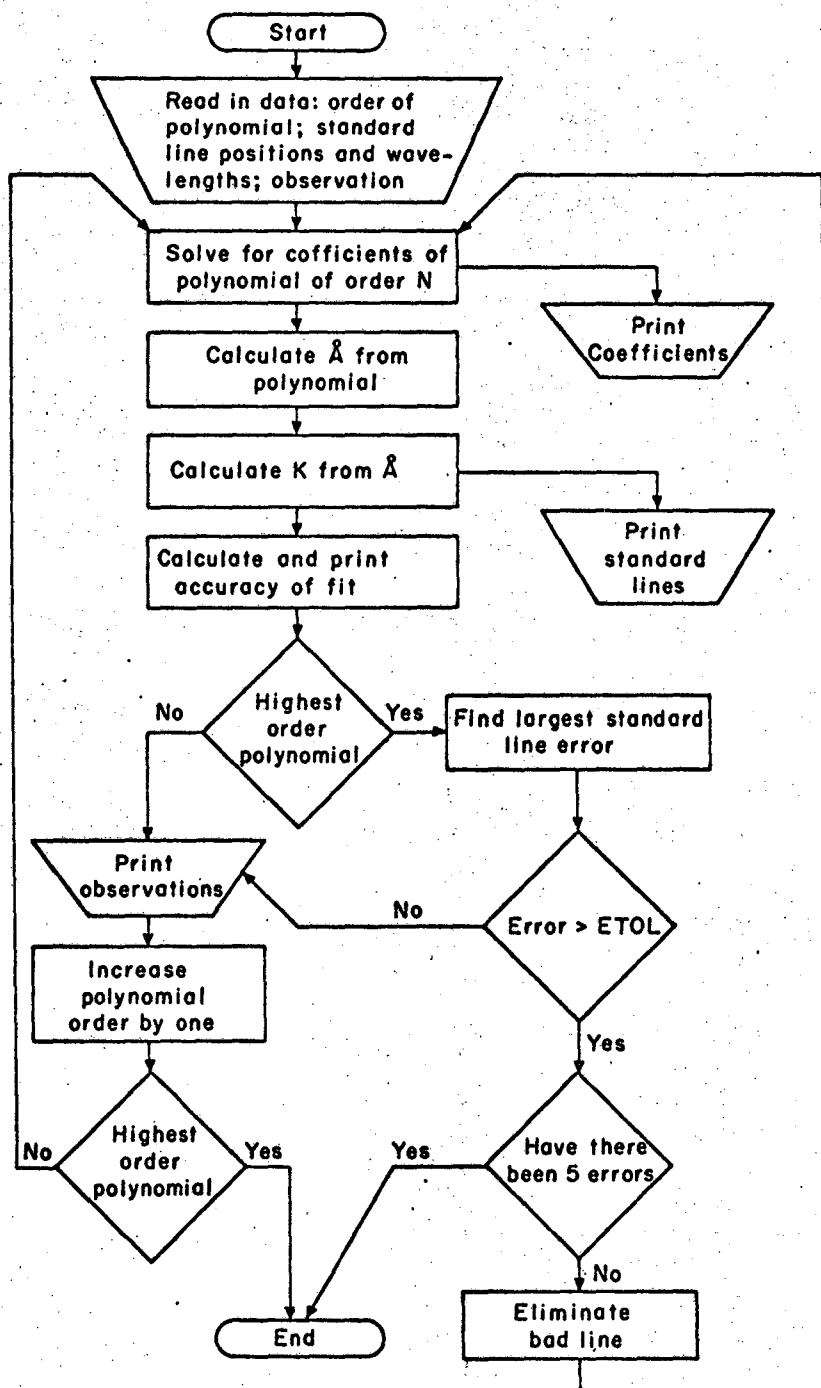
If there are  $I$  lines and positions to be used as standards, the equations of the following form must be simultaneously solved.

$$\begin{aligned} \sum_1^I \overset{\circ}{A}_i &= I c_0 + c_1 \sum_1^I x_i + c_2 \sum_1^I x_i^2 + \dots \\ \sum_1^I \overset{\circ}{A}_i x_i &= c_0 \sum_1^I x_i + c_1 \sum_1^I x_i^2 + c_2 \sum_1^I x_i^3 + \dots \\ \sum_1^I \overset{\circ}{A}_i x_i^2 &= c_0 \sum_1^I x_i^2 + c_1 \sum_1^I x_i^3 + c_2 \sum_1^I x_i^4 + \dots \end{aligned} \quad (11)$$

etc.

A flow diagram of program "Stand" is shown in Fig. 9. Table XV lists the method of data input. Several different order polynomial fits may be calculated in one computer run with one set of input data. In this work a linear fit was normally the initial order polynomial and a quadratic the





XBL 682-124

Fig. 9 Flow diagram of program "Stand"

Table XV. Data input for program "Stand".

Section	Column	Datum	Definition	Format
1.	1-5	N	lowest order of fit plus one. i.e., N = 2 for linear fit.	4I5
	6-10	NLAST	highest order of fit plus one.	
	11-15	NU	number of standard lines.	
	16-20	NTOT	total number of standard plus observed lines.	
2.	1-10	YY(I)	standard wavelengths (I = 1,NU).	F10.3
3.	1-10	X(I)	standard line positions (I = 1,NU).	F10.1
4.	1-10	X(J)	observed positions (J = NU+1,NTOT).	F10.1,
	11-15	COM(J)	comment in code for each observation.	F5.0
5.	1-10	ETOL	the tolerable error (true $\lambda$ .calc $\lambda$ ) in standard lines in $\text{\AA}$ .	F10.1

highest order used.

On the highest order polynomial the least accurate standard line (i.e. largest absolute value of the difference between the true wavelength and the wavelength calculated from the polynomial) is found. This line is eliminated if the error exceeds the tolerable error (ETOL) which was usually  $0.1 \text{ \AA}$  in this work. The calculations are then repeated until no standard lines have an error exceeding the tolerable error or until five lines have been determined to be bad. In this manner inaccurate measurements, improperly assigned standard lines or data input errors are eliminated without requiring the program to be rerun and without significantly affecting the accuracy of calculation of the observed lines wavelength.

The vacuum wave numbers in K for each observed line are obtained from the calculated wavelength by applying the formula of Edlen<sup>39</sup> with a small correction for water vapor.

This report was prepared as an account of Government sponsored work. Neither the United States, nor the Commission, nor any person acting on behalf of the Commission:

- A. Makes any warranty or representation, expressed or implied, with respect to the accuracy, completeness, or usefulness of the information contained in this report, or that the use of any information, apparatus, method, or process disclosed in this report may not infringe privately owned rights; or
- B. Assumes any liabilities with respect to the use of, or for damages resulting from the use of any information, apparatus, method, or process disclosed in this report.

As used in the above, "person acting on behalf of the Commission" includes any employee or contractor of the Commission, or employee of such contractor, to the extent that such employee or contractor of the Commission, or employee of such contractor prepares, disseminates, or provides access to, any information pursuant to his employment or contract with the Commission, or his employment with such contractor.

